

Sequential star formation at the periphery of the H II regions Sh 217 and Sh 219^{★ ★★}

L. Deharveng¹, A. Zavagno¹, L. Salas², A. Porras³, J. Caplan¹, and I. Cruz-González⁴

¹ Laboratoire d'Astrophysique de Marseille, 2 Place Le Verrier, 13248 Marseille Cedex 4, France
lise.deharveng@oamp.fr

² Observatorio Astronómico Nacional, IA-UNAM, Apdo. Postal 877, Ensenada, B.C. México
salas@astrocen.unam.mx

³ Instituto de Astronomía, UNAM, Apdo. Postal 3–72 (Xangari), 58089 Morelia, Mich. México
a.porras@astrosmo.unam.mx

⁴ Instituto de Astronomía, UNAM, Apdo. Postal 70-264, Cd. Universitaria, 04510 México, D.F. México
irene@astroscu.unam.mx

Received; accepted

Abstract. The H II regions Sh 217 and Sh 219 are textbook examples of a Strömgren sphere surrounded by an annular photodissociation region (PDR). The annular PDR is observed in both the 21 cm atomic hydrogen emission and the dust (PAH) emission near 8 μ m (MSX Survey).

An ultracompact radio continuum source is observed in the direction of the annular PDR, in both Sh 217 and Sh 219. *JHK* observations show the presence of highly reddened stellar clusters ($A_V \sim 20$ mag) in the directions of these radio sources. These clusters are also IRAS sources, of luminosities 22 700 L_\odot for Sh 217 and 5900 L_\odot for Sh 219. Each cluster contains at least one luminous star with an IR colour excess; the one in the Sh 219 cluster shows H α emission. The cluster associated with Sh 217 is almost spherical and contains luminous objects at its centre. The cluster associated with Sh 219 is elongated along the ionization front of this H II region.

We argue that these are ‘second-generation clusters’, which means that the physical conditions present in the PDRs, close to the ionization fronts, have favoured the formation of clusters containing massive objects. We discuss the physical mechanisms which may be at the origin of the observed triggered star formation.

Key words. H II regions – ISM: individual objects: Sh 217 – ISM: individual objects: Sh 219 – Stars: formation – Stars: early-type

1. Introduction

Most massive stars are observed associated with dense stellar clusters (Testi et al. 1999, 2001 and references therein). One possible interpretation of this observational fact is that the mechanism(s) for massive-star formation requires a cluster potential; the stars may form by coalescence from intermediate mass protostars (Bonnell et al. 1998, 2001, Stahler et al. 2000) or by accretion (Bernasconi & Maeder 1996, Norberg

& Maeder 2000, Behrend & Maeder 2001), at the centres of dense clusters. However, the observational data do not require such an interpretation; they are also compatible with the statistics of randomly assembled stars, with masses distributed according to the standard Initial Mass Function (Bonnell & Clarke 1999). Thus the mode of formation of massive stars is still debated. It is an important observational challenge to identify the progenitors of such stars and to characterize the physical conditions required to form them or the protoclusters.

Dobashi et al. (2001) have compiled a list of about 500 molecular clouds harbouring IRAS point sources with colours typical of protostars. Their study shows that protostars in clouds associated with H II regions are more luminous than those in clouds far from H II regions, thus highlighting the part played by H II regions in the formation of massive objects (stars or clusters). Observational evidence that H II regions are effi-

Send offprint requests to: L. Deharveng

[★] Based on observations done at the Observatorio Astronómico Nacional at San Pedro Mártir, México, and at the Observatoire de Haute-Provence, France.

^{★★} Tables 3 and 4 are available only at the CDS, via anonymous ftp to cdsarc.u-strasbg.fr (130.79.128.5) or via [http://cdsweb.u-strasbg.fr/cgi-bin/qcat?J/A+A/\(vol\)/\(page\)](http://cdsweb.u-strasbg.fr/cgi-bin/qcat?J/A+A/(vol)/(page))

cient sites of *second-generation* star formation is presented by Elmegreen (1998). Several physical mechanisms, discussed by Whitworth et al. (1994) and Elmegreen (1998), have been proposed to account for triggered star formation at the periphery of H II regions. These mechanisms depend on the high pressure in the ionized gas and on the expansion of the H II region: i) Star formation may result from the radiation-driven implosion of a pre-existing molecular clump: cometary globules are formed, surrounded by optically bright rims (Bertoldi 1989, Lefloch & Lazareff 1994). Indeed, star formation is observed at the centre of these globules (Lefloch et al. 1997, Sugitani et al. 2000 and references therein, Ogura et al. 2002). ii) Or, as described in the model of Elmegreen and Lada (1977, 1978; see also Whitworth et al. 1994), a compressed layer of high-density neutral material forms between the ionization front and the shock front preceding it in the neutral gas, and star formation occurs when this layer becomes gravitationally unstable.

We present here the case of the two H II regions Sh 217 and Sh 219, with their nearby associated clusters. Their simple morphology may help us to understand the process of sequential star formation possibly at work here. Each region appears to be a Strömgren sphere centred on a single exciting star, and surrounded by an annular photodissociation region (PDR). In each case a young cluster, containing at least one massive star, is observed at one position on the PDR annulus, like a brilliant on a ring. In Sect. 2 we describe the two H II regions, what is known about their exciting stars and the morphology of the photoionized and photodissociated zones. In Sect. 3 we present our near-IR observations of these newly-discovered young clusters. In Sect. 4 we discuss the process of sequential star formation in the light of what is observed in Sh 217 and Sh 219. Conclusions are drawn in Sect. 5.

2. Description of the H II regions

Sh 217 and Sh 219 are optically visible H II regions (Sharpless 1959) separated by some 45'. The J2000 coordinates of their central exciting stars are, for Sh 217, $\alpha = 4^{\text{h}}58^{\text{m}}45^{\text{s}}.4$, $\delta = +47^{\circ}59'55''$ and, for Sh 219, $\alpha = 4^{\text{h}}56^{\text{m}}10^{\text{s}}.5$, $\delta = +47^{\circ}23'34''$.

2.1. The distances

Although Sh 217 and Sh 219 are seen in projection at the edge of the supernova remnant HB9 (G160.9+2.6), these objects are not related to HB9, which is at a distance of about 1.2 kpc (Leahy & Roger 1991) whereas Sh 217 and Sh 219 have distances between 4 and 6 kpc. As we shall see, it is not clear whether Sh 217 and Sh 219 lie at the same distance.

In the following we discuss the photometric distances of their exciting stars.

The main exciting star of Sh 219 is of spectral type B0V, with $V=12.10$ and $B - V=0.53$ (Georgelin et al. 1973, Moffat et al. 1979, Lahulla 1987). Using the colour calibration of Schmidt-Kaler (1982) we estimate a visual extinction of 2.57 mag. The calibrations of Vacca et al. (1996) and of Humphreys & McElroy (1984) for the absolute magnitude of a B0V star lead to distance estimates of 5.6 kpc and 4.6 kpc, respectively.

Table 1. Kinematic information on Sh 217 and Sh 219

	V_{LSR} (km s ⁻¹)		references
	Sh 217	Sh 219	
CO	-20.5	-24.5	Blitz et al. 1982
CO	-18.1	-25.0	Wouterloot & Brand 1989
CO	-18.2		Jackson & Sewall 1982
H I	-17	-23	Roger & Leahy 1993
H α	-20.4	-31.0	Fich et al. 1990

(The absolute magnitude is particularly uncertain for this spectral type.)

The spectral type of the main exciting star of Sh 217 is uncertain – O9.5V, B0V or O8V according to Georgelin et al. (1973), Moffat et al. (1979) and Chini & Wink (1984) respectively; consequently its distance is very uncertain. In Sect. 2.3 we explain why we favour an O9V or later spectral type. Assuming O9V and using the absolute magnitude calibrations of Vacca et al. (1996) or of Schmidt-Kaler (1982) (which are not very different), its observed magnitude $V=11.34$ and colour $B - V=0.40$ correspond to a visual extinction of 2.20 mag and a distance in the range 5.18–5.35 kpc.

Thus the distance of Sh 219 is uncertain because of the uncertainty in the absolute magnitude of a B0V star, and the distance of Sh 217 is uncertain because of the uncertainty in the spectral type of its exciting star.

The kinematic distances deduced from the velocities of the associated molecular material (Table 1) by using the Galactic rotation curve of Brandt & Blitz (1993) are 5.2 kpc for Sh 217 and 4.2 kpc for Sh 219.

Given all these uncertainties, we adopt, in the following discussion, a distance of 5.0 ± 0.8 kpc for both Sh 217 and Sh 219.

2.2. The morphology of the H II regions

Sh 219, in Fig. 1a, is a prototypical Strömgren sphere: in the optical it appears to be a nearly spherical H II region centred on its exciting star. In the radio continuum, shown in Fig. 1b, it also appears almost circular, of diameter 4.4 pc (3') if situated at 5 kpc (Fich 1993 and references therein; Leahy 1997). The 1.4 GHz radio continuum (ionized gas) map from the NVSS survey (Condon et al. 1998) shows a slight asymmetry – an extension of the emission towards the south-west. Leahy (1997) has detected a non-resolved radio source in this direction, as shown in Fig. 1b; the J2000 coordinates of this source (estimated from Leahy's map) are: $\alpha = 4^{\text{h}}56^{\text{m}}02^{\text{s}}.2 \pm 0^{\text{s}}.4$, $\delta = +47^{\circ}23'06'' \pm 4''$. Sh 219's electron density estimated from the intensity ratio of the [O II] 3726–3727 Å doublet is rather low – ~ 170 cm⁻³ (Deharveng et al. 2000) – and its rms electron density estimated from the radio continuum emission is 55 cm⁻³ (Roger & Leahy 1993).

However, a circular appearance does not prove spherical symmetry; a champagne-model H II region (Tenorio-Tagle 1979) viewed face-on would appear symmetric for an observer situated on its axis. In the case of Sh 219, the champagne model is suggested by comparison of the radial velocities obtained for the ionized gas and for the associated molecular material. Table 1 shows that the ionized gas flows away from the molec-

ular cloud, more or less in the direction of the observer, with a velocity of $\sim 6.5 \text{ km s}^{-1}$, in agreement with the predictions of the champagne model.

Sh 217, in Fig. 2a, is somewhat elliptical, with outer dimensions of $10 \text{ pc} \times 14 \text{ pc}$. Its south-west part is the brightest, both at optical and radio wavelengths. In the radio continuum, in Fig. 2b, it appears as a half-shell surrounding the exciting star (Fich 1993, Roger & Leahy 1993, Condon et al. 1998). Here again an ultracompact radio source lies at its south-west periphery (Fig. 2b – it is unresolved with a resolution of $43''$); its J2000 coordinates are: $\alpha = 4^{\text{h}}58^{\text{m}}30^{\text{s}}.1$, $\delta = +47^{\circ}58'34''$. Sh 217 is a low density H II region, with an electron density of $\sim 50 \text{ cm}^{-3}$ deduced from the [O II] lines ratio, and of 20 cm^{-3} from the radio emission. The shell morphology of Sh 217 may also be the signature of a champagne model. This morphology indicates that the electron density is higher farther from the star: in the champagne model the highest electron densities are found at the borders of the cavity carved out of the high-density neutral material. However, in Sh 217, the velocities of the ionized gas and of the neutral material are similar (Table 1); this suggests that, if an ionized flow exists, there is a large angle between the mean direction of flow and the line of sight.

2.3. The exciting stars

Absolute integrated line fluxes of Sh 217 and Sh 219 in a number of nebular emission lines were measured through a circular diaphragm of diameter 4.5 by Caplan et al. (2000). The He^+/H^+ ratios obtained for these H II regions are rather low – 0.061 and 0.041 respectively – indicating that not all the helium is ionized; the O^{++} emission is very faint, with O^{++}/O ratios of 5×10^{-2} and 6×10^{-3} respectively (Deharveng et al. 2000). Thus, as regards their He^+ and O^{++} emission, Sh 217 and Sh 219 appear to be low-excitation regions, very similar to Sh 153, Sh 168 and Sh 211, which are ionized by O9.5V, O9V and O9V stars respectively. Also, Sh 219 is of lower excitation than Sh 217. All this is consistent with a B0V spectral type for the main exciting star of Sh 219, and suggests a slightly earlier spectral type, possibly O9.5V or O9V, for the exciting star of Sh 217.

Sh 217 and Sh 219 are thermal radio continuum sources. Their flux densities, measured at 1.46 GHz (Fich 1993, Roger & Leahy 1993), are in the ranges 400–472 mJy and 130–160 mJy respectively. We have used eq. 1 of Simpson & Rubin (1990) to determine the number of Lyman continuum photons emitted per second by their exciting stars. Assuming a distance of 5 kpc, helium ionic abundances of 0.06 for Sh 217 and 0.04 for Sh 219 and an electron temperature of 9200 K (Deharveng et al. 2000), we obtain $\log N_{\text{Lyc}} = 48.0$ for Sh 217 and 47.5 for Sh 219. According to Schaerer & de Koter (1997) these Lyman continuum fluxes indicate exciting stars of spectral types B0V for Sh 217 and cooler than B0.5V for Sh 219. This is somewhat cooler than the spectral types discussed in Sect. 2.1; perhaps not all emitted Lyman continuum photons are detected, as is expected in the case of a champagne model where the emission of the low-density extended ionized component would probably not be detected. However, the effective temperature and

thus the Lyman continuum flux of massive stars are still subject to revision (Martins et al. 2002), so that a difference of one subclass is probably not significant.

2.4. The photodissociation regions around Sh 217 and Sh 219

Sh 217 and Sh 219 have been mapped in H I at 21 cm, with an angular resolution of $1'.0 \times 1'.4$ (Roger & Leahy 1993). Both H II regions show prominent photodissociation regions (PDRs) surrounding the ionized zones.

Figure 2c shows the H I emission associated with Sh 217, integrated from -15.1 to -20.1 km s^{-1} (V_{LSR}), superimposed on a DSS2-red frame of this region. An almost complete ring of H I emission surrounds the H II region. The ring is broad, with a typical radial extent of 5–10 pc and with a peak column density of $3 \times 10^{20} \text{ cm}^{-2}$. The ring contains about $650 M_{\odot}$ of atomic hydrogen, with a mean density of 15 atoms cm^{-3} .

Figure 1c shows the H I emission associated with Sh 219, integrated from -21.7 to -26.6 km s^{-1} , superimposed on a DSS2-red frame. The surrounding H I emission is less symmetric than for Sh 217, with a pronounced deficiency on the western side, in the direction of the stellar cluster discussed in Sect. 3.2. This incomplete ring has a peak column density of $1.8 \times 10^{20} \text{ cm}^{-2}$, and contains about $86 M_{\odot}$ of atomic hydrogen with a mean density of 9 atoms cm^{-3} .

We have searched for Sh 217 and Sh 219 in the MSX infrared survey (Egan et al. 1999; this survey has an angular resolution of $18''$ in band A, centred at $8.3 \mu\text{m}$). These H II regions have counterparts in MSX's band A, where they appear as semi-circular emission rings (Figs 1b and 2b). In each case an 'MSX point source' is observed in the direction of the ring. Their positions and fluxes are given in Table 2.

The MSX band A covers the $6.8\text{--}10.8 \mu\text{m}$ range (at half transmission). It contains the $7.7 \mu\text{m}$ and $8.6 \mu\text{m}$ emission bands, often attributed to polycyclic aromatic hydrocarbons (PAHs; Léger & Puget 1984, Alamandola et al. 1985; see also Verstraete et al. 2001 for a discussion of the origin of these bands), and an underlying continuum attributed to very small grains. PAHs cannot survive in ionized regions. This is clearly demonstrated by the ISO spectra obtained at different positions in the M 17 field by Cesarsky et al. (1996; their fig. 2); the spectrum obtained in the direction of the ionized region is dominated by a continuum, rising strongly with increasing wavelength, whereas that obtained in the direction of the neutral PDR shows the PAH emission bands superimposed on a continuum. In the PDR, the PAHs absorb the strong UV radiation leaking from the H II region, are heated (possibly ionized), and radiate in the PAH bands. This is most probably the origin of the band A emission forming the rings surrounding the Sh 217 and Sh 219 H II regions.

The MSX point sources coincide with the ultracompact radio sources and the infrared clusters discussed in this paper. These 'point sources' are resolved: that associated with Sh 217 has circular isophotes and, after correction for the PSF, a FWHM of $25''$ (0.6 pc); that associated with Sh 219 is elongated along the ionization front, with a FWHM perpendicular

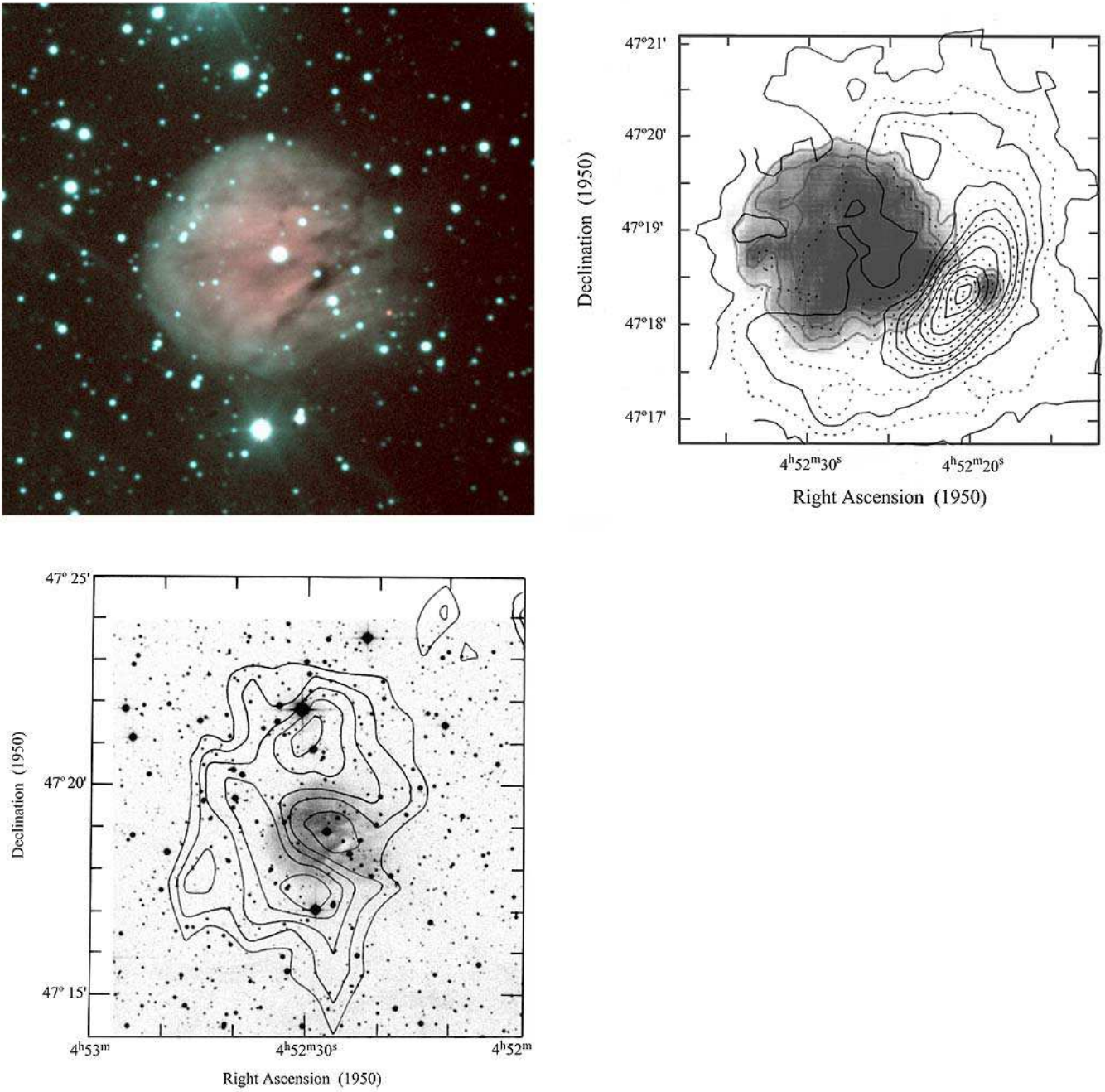


Fig. 1. **a)** Composite colour image of Sh 219 in the optical; pink corresponds to the $H\alpha$ 6563 Å emission, and turquoise to the $[S II]$ 6717–6731 Å emission (the $[S II]$ emission comes from low-excitation ionized zones; it is enhanced close to the ionization fronts). These frames were obtained with the 120 cm telescope of the Observatoire de Haute-Provence (exposure times 1 h and 2 h respectively). The size of the field is $5'.6 \times 5'.2$. North is up and east is to the left. **b)** Sh 219 in the IR and radio continuum. The black contours (solid and dotted), drawn from the MSX 8.3 μm image, are superimposed on the grey-scale 1.42 GHz continuum map of Leahy (1997). The MSX radiance contours range from 1 to $14 \times 10^{-6} \text{ W m}^{-2} \text{ sr}^{-1}$. Note the half-ring of dust emission surrounding the $H II$ region. **c)** Integrated $H I$ emission associated with Sh 219 covering the LSR radial velocity range from -21.7 km s^{-1} to -26.6 km s^{-1} (from Roger & Leahy 1993). The $H I$ contours are superimposed on the DSS2-red frame of Sh 219

to the front of $11''$ (0.25 pc). These MSX point sources are also IRAS point sources. Table 2 gives their IRAS identifications, fluxes and luminosities (calculated according to Chan & Fich 1995). IRAS 04547+ 4753, associated with Sh 217, has the characteristic colours of an ultracompact $H II$ region (Wood &

Churchwell 1989). Its low-resolution IRAS spectrum shows a red continuum with no PAH features (Chen et al. 1995). Its luminosity is that of a cluster containing a few early B stars. The colours and luminosity of IRAS 04523+4718, associated with Sh 219, are more characteristic of intermediate mass protostars

(e.g. Herbig Be stars) than of ultracompact H II regions. No maser emission has been detected in the direction of these two IRAS sources (Wouterloot et al. 1993, MacLeod et al. 1998, Szymczak et al. 2000).

2.5. The molecular material associated with Sh 217 and Sh 219

Sh 217 has been mapped in ^{12}CO and ^{13}CO (1–0 transition), with a resolution of $65''$, by Jackson & Sewall (1982). The $4100 M_{\odot}$ of molecular material associated with Sh 217 is located mainly in three components. The main component is associated with the ultracompact H II region and the MSX point source. In this direction, the mean molecular hydrogen density is 730 cm^{-3} , and the column density $N(^{13}\text{CO})$ reaches $9 \times 10^{15} \text{ cm}^{-2}$ (corresponding to $N(\text{H}_2) \sim 4.5 \times 10^{21} \text{ cm}^{-2}$ according to Jackson & Sewall). The low angular resolution does not allow us to see any details connected with the ionization front or with the cluster. The visual extinction corresponding to this column density, $A_V \sim 4.5 \text{ mag}$ (Thronson et al. 1985), is much smaller than that observed for individual stars in the cluster (Sect. 3), suggesting that the dust/gas ratio is anomalous or, more probably, that dense structures are present but not observed. Two fainter components are observed in the direction of the H II region (Jackson & Sewall 1982). Comparison of the H I and CO emission maps shows a remarkable anti-correlation between these two emissions.

Very little molecular material is found to be associated with Sh 219 (Huang & Thaddeus 1986).

3. Star formation associated with Sh 217 and Sh 219

3.1. Near-IR observations

Frames of these regions in J , H and K' have been obtained in October 2000 at the 2.12-m telescope of the Observatorio Astronómico Nacional at San Pedro Mártir, Baja California, México. We have used the CAMILA camera (Cruz-González et al. 1994) with the f/4.5 focal reducer, which gives a scale of $0''.85$ per pixel and a field of $3'.6 \times 3'.6$. The observing and reduction techniques are as described in Deharveng et al. (1997).

Eighteen UKIRT standard stars, covering a large colour range ($-0.231 \leq J - K \leq +2.992$), were observed to determine the colour equations and zero points of the photometric system. In the following, all the magnitudes are given after transformation to the UKIRT system.

3.2. Results for Sh 219

Sh 219 was observed in October 2000 with total integration times of 750 s in each band. Our magnitude detection limits are of about 17.5 in J and 16.5 in H and K (corresponding to a threshold of 3σ ; 222 stars were measured in at least two bands, of which 142 were measured in all three bands. The J2000 coordinates of these stars, their K magnitudes and their $J - K$, $J - H$ and $H - K$ colours are given in Table 3. The uncertainty of each magnitude is generally smaller than 0.2 mag.

Table 3. Coordinates and JHK photometry of all the stars in a $3'.5 \times 3'.5$ field centred on Sh 219. This Table, available at the CDS, contains the following information. Column 1 gives the numbers of the stars, Columns 2 and 3 their X and Y tangential coordinates in arcminutes, Columns 4 through 9 their J2000 equatorial coordinates, Column 10 the K magnitude and Columns 11 through 13 the colours $J - K$, $J - H$ and $H - K$.

Figure 3a shows the K frame. The stars discussed in the text are identified by the same numbers as in Table 3. Figure 3b is a JHK colour composite image. This image shows the effects of extinction, the differences in colour of the stars mainly being due to differences in reddening. These figures show two important facts: i) a previously unreported cluster of reddened stars appears at the south-west periphery of the Sh 219 H II region; ii) the central exciting star of Sh 219, no. 194, appears isolated: no nearby red companions appear in K .

Figures 4a and 4b present respectively the K versus $J - K$ and the $J - H$ versus $H - K$ diagrams. Figure 4b shows that most of the stars appear to be reddened main-sequence stars, and thus Fig. 4a can be used to estimate their visual extinctions. Certain stars – nos 99, 102, 160, 179, 194, 204, 216 – are affected by a relatively small visual extinction (3–5 mag). This probably corresponds to the general interstellar extinction for the distance of Sh 219; these stars are probably unaffected by local extinction. The exciting star of Sh 219, no. 194, whose near-IR magnitudes are consistent with a B0V spectral type (see Sect. 2.1), belongs to this group. The case of stars 21, 34, 37 and 142 is not as clear. If these are main-sequence stars, they have a visual extinction in the 7.2–8.1 mag range; if situated at the distance of Sh 219, they are intrinsically luminous, and star no. 34 at least should ionize the surrounding medium and form an H II region. Such an H II region is detected neither in the DSS2-red survey nor in the radio continuum maps. Perhaps these stars are cool giants unrelated to the cluster; their positions in the $J - H$ versus $H - K$ diagram are compatible with this possibility. A number of stars – nos 82, 133, 139, 150, 158, 165, etc. – mostly located in the direction of the small cluster, have extinctions greater than 11 mag. Star 139, close to the centre of the cluster, is one of the brightest and most highly reddened objects, with $A_V \sim 24 \text{ mag}$. It is intrinsically brighter in K than no. 194, the exciting star of Sh 219. Star 139 displays a clear near-IR excess; it is probably still associated with very hot dust situated in an accreting disk or envelope, very close to the central object. The $H\alpha + [\text{S II}]$ colour image of Sh 219 (Fig. 1a) shows that star 139 is also an $H\alpha$ emission star (it is the only ‘pink star’ of the image). Star no. 139 cannot be the exciting star of the non-resolved radio continuum source, as it lies $18''$ away. Star 158, lying $1''$ from the radio source (visual extinction $\sim 11.5 \text{ mag}$), is a possibility.

The cluster observed at the south-west periphery of Sh 219 subtends an angle of about 60° with respect to the exciting star of Sh 219. The cluster is not spherical, but is elongated along the ionization front, suggesting that star formation was triggered by the passage of the front (see Sect. 4.4).

Table 2. MSX and IRAS observations of the point sources associated with Sh 217 and Sh 219

Source	$\alpha(2000)$	$\delta(2000)$	Flux (Jy)					$L_{\text{IR}} (L_{\odot})$
			8.3 μm	12 μm	25 μm	60 μm	100 μm	
MSX Sh 217	4 ^h 58 ^m 30.3	+47°58'33"	11.6					
IRAS04547+4753	4 ^h 58 ^m 29.7	+47°58'28"		10.42	82.03	359.80	367.30	22700
MSX Sh 219	4 ^h 56 ^m 03.9	+47°22'55"	1.25:					
IRAS04523+4718	4 ^h 56 ^m 04.0	+47°22'58"		3.30	5.21	81.70	304.70	5900

3.3. Results for Sh 217

The stellar cluster discovered at the periphery of Sh 217 has been studied in the near IR as part of a large survey of the Initial Mass Function in young clusters by Porras (2001) and Porras et al. (2000, 2002). *JHK* photometry and coordinates of 121 stars are presented here. Their coordinates and magnitudes are given in Table 4. The stars discussed in the text are identified on the *H* frame, in Fig. 5a.

Figure 5a shows an almost spherical cluster, with luminous objects at its centre; 90% of the stars in the cluster are enclosed in a circle of radius 1.1 pc. Figure 5b is a *JHK* colour composite image of this cluster and the surrounding stars. The image emphasizes the large variations of extinction among the stars in this field, especially among the massive objects in the direction of the centre of the cluster region.

The colour-magnitude diagram is presented in Fig. 6. The bright star 123, with $A_V=0.9$ mag, is probably a foreground star. Stars 24, 47, 99 and 117 have A_V in the range 2–4 mag, whereas stars 13, 14, 19, 36, 40, 45, 65, 107 and 118 are more reddened, with A_V from 5 to 11 mag. The two blue stars, nos 45 and 47 ($A_V \sim 5.6$ mag and 3.4 mag respectively), have been tentatively classified as B2V by Moffat et al. (1979) on the basis of their *UBV* photometry. The colour-magnitude diagram confirms that they are B stars, but probably of a later spectral type, in which case they are not the only ionization sources of the associated compact H II

The mean visual extinction of the cluster is about 8 mag. The western part of the cluster shows deeply embedded objects. Two red objects, nos 32 and 49, appear very luminous in *K*, as bright as B0V stars (Fig. 6). Assuming they are on the main sequence, their visual extinctions would be 15.5 mag and 19.1 mag respectively. However star 32 shows a near-IR excess, and thus is probably a Herbig Be star with less extinction. Star 49 presents no near-IR excess, but its *J* magnitude is uncertain (due to the high stellar density, the high background emission and the high extinction, the uncertainty in the colours of the faint objects in this cluster may be greater than 0.3 mag). These two stars probably contribute to the ionization of the associated compact H II region.

4. Discussion

4.1. How old are Sh 217 and Sh 219?

The dynamical ages of Sh 217 and Sh 219 can be estimated by using the model by Dyson & Williams (1980) of an H II region expanding in a homogeneous medium. An unknown parameter here is the density of the medium into which the H II

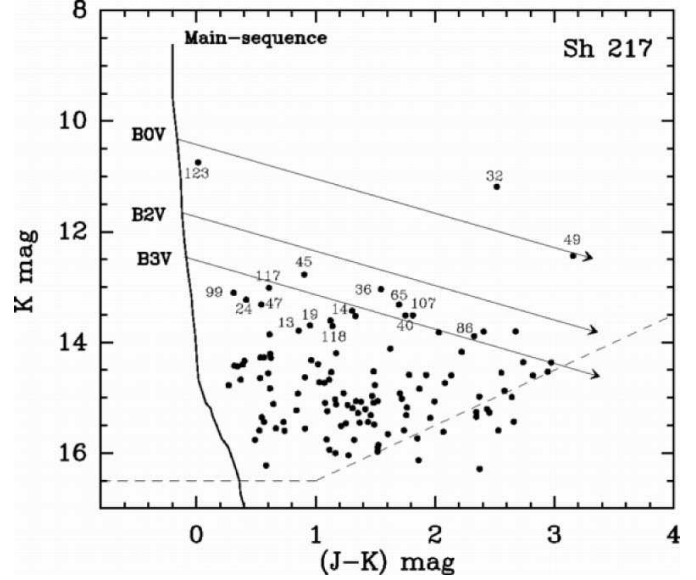


Fig. 6. The *K* versus (*J* – *K*) magnitude-colour diagram of stars in the Sh 217 field. Main sequence, detection limits and reddening as in Fig. 4a

Table 4. Coordinates and *JHK* photometry of all the stars in a 3.1 × 3.2 field centred on Sh 217. This Table, available at the CDS, contains the following information. Column 1 gives the numbers of the stars, Columns 2 and 3 their *X* and *Y* tangential coordinates in arcminutes, Columns 4 through 9 their J2000 equatorial coordinates, Column 10 the *K* magnitude and Columns 11 through 13 the colours *J* – *K*, *J* – *H* and *H* – *K*.

regions evolve. Sh 219 is excited by a B0V star, which emits 1.25×10^{48} ionizing photons per second (Vacca et al. 1996, Schaerer & de Koter 1997). If expanding into a homogeneous medium of 10^3 cm^{-3} , Sh 219's present radius of 2.2 pc would correspond to an age of 4.4×10^5 years and an expansion velocity of 2.7 km s^{-1} . If expanding into a lower density medium, for example 10^2 cm^{-3} , it would be much younger – 6.6×10^4 years – and would be expanding with the higher velocity of 8.5 km s^{-1} .

Sh 217 is twice as large as Sh 219. Given that it is excited by a star emitting 2.0×10^{48} ionizing photons per second, its larger size implies that it is either older than Sh 219 or that it has developed in a lower density medium. For example, expanding into a homogeneous medium of 10^3 cm^{-3} , its dynamical age would be 1.4×10^6 years and its present expansion velocity 1.8 km s^{-1} . Alternatively, an age of 4.4×10^5 years implies

expansion in a 150 cm^{-3} medium, with a present expansion velocity of 4.6 km s^{-1} .

Most probably the exciting stars of these regions formed in high density molecular cores but, later, the associated H II regions evolved within a lower density medium. Furthermore, all of these estimations assume that both the H II region and its surrounding medium are spherically symmetric around the exciting star. As we have seen in Sect. 2.2, there is some kinematic evidence that Sh 219 is undergoing a champagne flow, and the shell morphology of Sh 217 may also be the signature of a champagne model. If these H II regions correspond to a champagne model, they are older than estimated previously, and their expansion velocities lower. This would explain why no expansion is observed in the H I rings surrounding these H II regions (Roger & Leahy 1993).

The relative sizes and masses of the H II regions and of their atomic PDRs are also age indicators. They depend mainly on the exciting stars, on the ambient density, on the amount of photoabsorption by dust grains, and are functions of the time. As a region expands, the dissociation rate of molecular hydrogen behind the ionization front, which depends on the UV energy density, decreases. As a consequence, the dissociation front is eventually caught up by the ionization front, and the H I zone disappears (Rogers & Dewdney 1992).

According to the observations, the ratios of the sizes and masses of the photoionized and photodissociated regions of Sh 217 and Sh 219 are respectively 1.9 and 2.2 for $R_{\text{H I}}/R_{\text{H II}}$, and 1.9 and 2.5 for $M_{\text{H I}}/M_{\text{H II}}$. Comparison with the non-stationary models of Roger & Dewdney (1992) indicates that Sh 217 and Sh 219 cannot have developed in a medium as dense as 10^3 cm^{-3} , but most probably in a medium of density $\leq 30 \text{ cm}^{-3}$. But then, the ages predicted by the models are incredibly young (a few 10^4 years; Roger & Leahy 1993).

Dust absorption is important. This effect reduces the size of the ionized and atomic zones, as well as the $R_{\text{H I}}/R_{\text{H II}}$ and $M_{\text{H I}}/M_{\text{H II}}$ ratios; dust absorption is more important in the photodissociation zone, as shown by the models of Diaz-Miller et al. (1998). Weingartner & Draine (2001) have proposed that the stellar radiation pressure drives the grains through the gas, leading to an increase of the dust-to-gas ratio in the PDR. Large amounts of dust in the PDRs of Sh 217 and Sh 219 could account, at least partly, for the low values of the observed ratios. This last effect, not taken into account in the models, as well as the possibility of a clumpy PDR, result in very uncertain age determinations.

4.2. The great similarity of Sh 217 and Sh 219

Although Sh 217 and Sh 219 are separated in projection by some 65 pc, they are similar in many respects: i) Sh 217 and Sh 219 appear as spherical (or hemispherical) H II regions, excited by a single central star (see Sect. 2.3); ii) the H II regions are surrounded by annular H I zones of low column density (accounting for less than 0.5 mag of visual extinction); iii) a cluster is observed at one position at the periphery of each H II region, in the direction of the PDR, in an area of high dust emission very close to the ionization front; iv) these clusters are

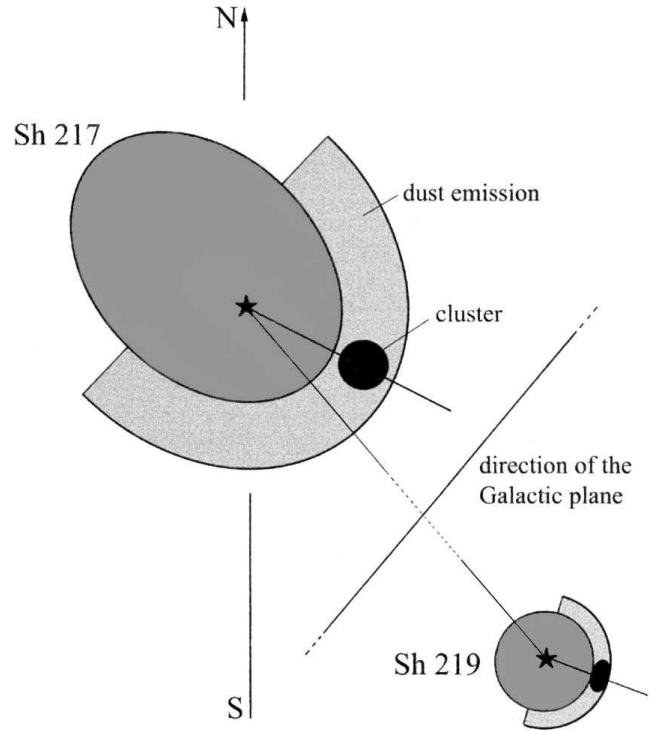


Fig. 7. A schematic view of the respective positions and dimensions of the Sh 217 and Sh 219 H II regions, their half-rings of PAHs emission, and the associated embedded clusters. The distance between Sh 217 and Sh 219 is not to scale

reddened, with some objects affected by a visual extinction up to 20 mag, and they contain massive stars, which ionize compact H II regions; v) the offset direction of the cluster from the exciting star of the extended H II region is the same, to within a few degrees, for Sh 217 and Sh 219: these directions are nearly perpendicular to the Galactic plane. Fig. 7 summarises this situation.

A difference between the two H II regions is that very little molecular material seems to be associated with Sh 219, contrary to the situation in Sh 217.

4.3. Sequential star formation?

As far as we can see from the present observations, the exciting stars of Sh 217 and Sh 219 are isolated massive stars: no nearby luminous companions appear on the *K* frames of these regions as they do, for example, for the exciting stars of Sh 138 (Deharveng et al. 1999). Have these stars formed in isolation?

If we assume that the exciting stars of Sh 217 and Sh 219 formed in a common cluster and were both subsequently ejected after internal dynamical interactions $t(10^6)$ years ago, their current separation (65 pc in projection) implies space velocities larger than $32/t \text{ km s}^{-1}$. This value seems somewhat high for massive stars. Also, if the stellar velocity dispersion is 2 km s^{-1} (as in the Orion cluster, Jones & Walker 1988), then t million years after its formation this cluster should have a diameter of $2.1 \times t \text{ pc}$. We have examined the DSS and 2MASS surveys, trying to detect this cluster by eye from an over-

density of stars at some location between Sh 217 and Sh 219, without success.

Another possibility is to assume that the exciting stars of Sh 217 and Sh 219 formed in their respective peripheral clusters which we observe today, and were subsequently ejected from these clusters. There is a finite probability that the exciting star of each H II region formed in the cluster and was ejected; but the probability that, being ejected, each forms an H II region with a radius just equal to the star-cluster distance is very low. This requires that, for each region, the ejection velocity be, by chance, equal to the radius of the H II region divided by its age; furthermore, as the two H II regions present the same configuration (same position angle $\pm 10^\circ$ of the cluster with respect to the H II region's exciting star), the direction of the ejection must be, by chance, the same for both regions!

Thus the clusters observed at the periphery of the Sh 217 and Sh 219 H II regions are most probably second-generation clusters.

4.4. Physical processes of sequential star formation

In the following we assume that we are observing second-generation clusters, situated at the present time inside the PDRs. The best way to test this idea would be to compare the age of the H II regions and that of the clusters but, as we are dealing with young massive objects evolving rapidly, it is almost impossible to estimate ages accurately enough to allow comparison.

According to the model of Elmegreen & Lada (1977; cf. also Whitworth et al. 1994), as the H II region expands, a thin layer of compressed neutral material forms between the ionization front and the shock front that precedes it in the neutral material. This layer may eventually become gravitationally unstable, fragment and form stars. This may be the configuration observed in Sh 217 and Sh 219. The elongation along the ionization front of the cluster associated with Sh 219 is a strong argument in favour of this model.

The H I zones surrounding Sh 217 and Sh 219 do not correspond to such a compressed layer. Whitworth et al. (1994) have shown that the layer fragments when its column density reaches $\sim 6 \times 10^{21} \text{ cm}^{-2}$. This is higher than the observed column density in the H I rings by a factor ~ 20 . Thus if such a compressed layer exists it is most probably molecular. High angular resolution observations of the molecular material associated with Sh 217 and Sh 219 would confirm or infirm the existence of this layer. If this model were confirmed, we would need to explain how a wide low-density H I zone as well as a thin layer of dense molecular material can surround these H II regions. Can a clumpy PDR solve this problem (with dense molecular clumps surrounded by low-density atomic gas)?

A problem with Elmegreen & Lada's model concerns the ages and sizes of the H II regions. Using the same numbers as in Sect. 4.1 to estimate the ages of Sh 217 and Sh 219, we find that these H II regions (especially Sh 219) are too young for the layer to become gravitationally unstable and form stars. If the H II regions satisfy the champagne model, they are older; can this particular geometry help solve this problem? Another

possibility is that the shocked expanding layer, prior to the beginning of the instability, collides with a pre-existing molecular core. Star formation would take place at the interface between the layer and the cloud core. This would explain why only one site of star formation is observed along each ring, and could explain why the young cluster of Sh 217 is observed at the border of both the H II region and the main molecular core.

Whitworth et al. (1994) have shown that, when the fragmentation of the shocked layer starts at the border of the expanding H II region, the mass of the fragments 1) depends very little on the ionizing flux, 2) varies as $n^{-\frac{5}{11}}$, where n is the density of the surrounding medium and 3) depends strongly on the turbulence in the shocked layer, and thus on the temperature T of the gas in this layer, varying as $T^{\frac{20}{11}}$. PDR models (see Hollenbach & Tielens 1997 and references therein) predict high temperatures for the gas, as high as 1000 K close to the ionization fronts. This situation favours the formation of massive fragments susceptible to form massive stars and possibly clusters.

Sh 217 and Sh 219 are not the only such objects. We have used the MSX survey to search for annular (or semi-annular) dust emission structures surrounding small H II regions having MSX point sources in the direction of the dust rings. We have found about twenty such objects (Deharveng et al., in preparation). Most of these MSX point sources are also IRAS point sources, and some are associated with embedded clusters. These sources are possibly second-generation clusters.

5. Conclusions

Sh 217 and Sh 219 are textbook examples of the appearance of an H II region excited by a central isolated massive star (a Strömgren sphere) and its associated photodissociation region. We have argued that the physical conditions present in these photodissociation regions have favoured the formation of second-generation clusters containing massive stars. The case of these two regions is not unique.

However, as often, an apparently simple configuration turns out to be more complicated than anticipated. Here the H II regions are possibly non-spherical, and are best described by a champagne model; the H I PDR is possibly inhomogeneous. We have presented observational evidence suggesting that sequential star formation occurs at the periphery of Sh 217 and Sh 219. However, we are still unable to demonstrate what physical process is at work – whether gravitational instability of the shocked layer surrounding the H II regions or collision of this expanding layer with a pre-existing molecular core. We also need to determine which physical conditions allow the formation of clusters: high temperature and/or inhomogeneity of the PDR, slow evolution of non-spherical H II regions, etc. High resolution molecular observations of the PDRs of these regions should allow us to answer some of these questions.

Acknowledgements. We would like to thank the San Pedro Mártir Observatory staff for their support during the observations. D. Gravallon is thanked for the optical frames of Sh 217 and Sh 219 that he obtained for this study at the Observatoire de Haute-Provence. The MSX Survey has been particularly useful, and we thank M. Egan

and S. Carey for their help. The referee's useful comments are greatly appreciated. This publication makes use of the NRAO VLA Sky Survey, and of the NASA/IPAC Infrared Science Archive, which is operated by the Jet Propulsion Laboratory, California Institute of Technology, under contract with the National Aeronautics and Space Administration. This research has made use of the Simbad astronomical database operated at CDS, Strasbourg, France. L.S. and A.P. thank the Université de Provence and the Laboratoire d'Astrophysique de Marseille for providing one month of financial support in Marseille.

References

- Allamandola, L.J., Tielens, A.G.G.M., Barker, J.R., 1985, *ApJ* 290, L25
- Behrend, R., Maeder, A., 2001, *A&A* 373, 190
- Bernasconi, P.A., Maeder, A., 1996, *A&A* 307, 829
- Bertoldi, F., 1989, *ApJ* 346, 735
- Blitz, L., Fich, M., Stark, A.A., 1982, *ApJS* 49, 183
- Bonnell, I.A., Bate, M.R., Zinnecker, H., 1998, *MNRAS* 298, 93
- Bonnell, I.A., Bate, M.R., Clarke, C.J., Pringle, J.E., 2001, *MNRAS* 323, 785
- Bonnell, I.A., Clarke, C.J., 1999, *MNRAS* 309, 461
- Brand, J., Blitz, L., 1993, *A&A* 275, 67
- Caplan, J., Deharveng, L., Pena, M., Costero, R., Blondel, C., 2000, *MNRAS* 311, 317
- Cesarsky, D., Lequeux, J., Abergel, A., Perault, M., Palazzi, E., Madden, S., Tran, D., 1996, *A&A* 315, L309
- Chan, G., Fich, M., 1995, *AJ* 109, 2611
- Chen, P.S., Gao, H., Xiong, G.Z., 1995, *ApJS* 100, 389
- Chini, R., Wink, J.E., 1984, *A&A* 139, L5
- Condon, J.J., Cotton, W.D., Greisen, E.W., Yin, Q.F., Perley, R.A., Taylor, G.B., Broderick, J.J., 1998, *AJ* 115, 1693
- Cruz-González, I., Carrasco, L., Ruiz, E., Salas, L., Strutskie, M., Meyer, M., Sotelo, P., Barbosa, F., Gutierrez, L., Iriarte, A., Cobos, F., Bernal, A., Sanchez, B., Valdez, J., Argelles, S., Conconi, P., 1994, *SPIE* 2198, 774 (Instrum. in Astronomy VIII)
- Deharveng, L., Zavagno, A., Cruz-González, I., Salas, L., Caplan, J., Carrasco, L., 1997, *A&A* 317, 459
- Deharveng, L., Zavagno, A., Nadeau, D., Caplan, J., Petit, M., 1999, *A&A* 344, 943
- Deharveng, L., Pena, M., Caplan, J., Costero, R., 2000, *MNRAS* 311, 329
- Diaz-Miller, R.I., Franco, J., Shore, S.N., 1998, *ApJ* 501, 192
- Dobashi, K., Yonekura, Y., Matsumoto, T., Momose, M., Sato, F., Bernard, J.-P., Ogawa, H., 2001, *PASJ* 53, 85
- Dyson, J.E., Williams, D.A., 1980, *The Physics of the Interstellar Medium* (Manchester Univ. Press, Manchester)
- Egan, M.P., Price, S.D., Moshir, M.M., Cohen, M., Tedesco, E., Murdock, T.L., Zweil, A., Burdick, S., Bonito, N., Gugliotti, G.M., Duszak, J., 1999, *The Midcourse Space Experiment Point Source Catalog Version 1.2 Explanatory Guide*, AFRL-VS-TR-1999-1522, Air Force Research Laboratory
- Elmegreen, B.G., 1998, in *ASP Conference series* 148, ed. C.E.E. Woodward, J.M. Shull & H.A. Tronson, 150
- Elmegreen, B.G., Lada, C.J., 1977, *ApJ* 214, 725
- Elmegreen, B.G., Lada, C.J., 1978, *ApJ* 220, 1051
- Fich, M., Treffers, R.R., Dahl, G.P., 1990, *AJ* 99, 622
- Fich, M., 1993, *ApJSS* 86, 475
- Georgelin, Y.M., Georgelin, Y.P., Roux, S., 1973, *A&A* 25, 337
- Hollenbach, D.J., Tielens, G.G.M., 1997, *ARA&A* 35, 179
- Huang, J.-L., Thaddeus, P., 1986, *ApJ* 309, 804
- Humphreys, R.M., McElroy, D.B., 1984, *ApJ* 284, 565
- Jackson, P.D., Sewall, J.R., 1982, in *Regions of Recent Star Formation*, ed. R.S. Roger & P.E. Dewdney (D. Reidel), 221
- Jones, B.F., Walker, M.F., 1988, *AJ* 95, 1755
- Lahulla, J.F., 1987, *AJ* 94, 1062
- Leahy, D.A., Roger, R.S., 1991, *AJ* 101, 1033
- Leahy, D.A., 1997, *JRASC* 91, 127
- Lefloch, B., Lazareff, B., 1994, *A&A* 289, 559
- Lefloch, B., Lazareff, B., Castets, A., 1997, *A&A* 324, 249
- Léger, A., Puget, J.-L., 1984, *A&A* 137, L5
- MacLeod, G.C., Van der Walt, D.J., North, A., Gaylard, M.J., Galt, J.A., Moriarty-Schieven, G.H., 1998, *AJ* 116, 2936
- Martins, F., Schaerer, D., Hillier, D.J., 2002, *A&A* 382, 999
- Mathis, J.S., 1990, *ARAA* 28, 37
- Moffat, A.F.J., Fitzgerald, M.P., Jackson, P.D., 1979, *A&AS* 38, 197
- Norberg, P., Maeder, A., 2000, *A&A* 359, 1025
- Ogura, K., Sugitani, K., Pickles, A., 2002, *AJ* 123, 2597
- Porras, A., 2001, Ph.D. Thesis, INAOE (México)
- Porras, A., Cruz-González, I., Salas, L., 2000, in *33rd ESLAB Symposium: Star Formation from the Small to the Large Scale*, ed. F. Favata, A. Kaas & A. Wilson, 491
- Porras, A., Cruz-González, I., Salas, L., 2002, submitted to *ApJ*
- Roger, R.S., Dewdney, P.E., 1992, *ApJ* 385, 536
- Roger, R.S., Leahy, D.A., 1993, *AJ* 106, 31
- Schaerer, D., de Koter, A., 1997, *A&A* 322, 598
- Schmidt-Kaler, T., 1982, in *Landolt-Börnstein, New Series, Group VI, Vol. 2*, ed. K. Schaifers & H.H. Voigt (Berlin: Springer-Verlag), 1
- Sharpless, S., 1959, *ApJS* 4, 257
- Simpson, J.P., Rubin, R.H., 1990, *ApJ* 354, 165
- Sugitani, K., Tamura, M., Ogura, K., 1995, *AJ* 455, L39
- Sugitani, K., Matsuo, H., Nakano, M., Tamura, M., Ogura, K., 2000, *ApJ* 119, 32
- Stahler, S.W., Palla, F., Ho, P.T.P., 2000, in *Protostars and Planets IV*, ed. V. Mannings, A.P. Boss & S.S. Russell (Univ. Arizona Press), 327
- Szymczak, M., Hrynek, G., Kus, A.J., 2000, *A&AS* 143, 269
- Tenorio-Tagle, G., 1979, *A&A* 71, 59
- Testi, L., Palla, F., Natta, A., 1999, *A&A* 342, 515
- Testi, L., Palla, F., Natta, A., 2001, in *ASP Conference Series* 243, ed. T. Montmerle & P. André, 377
- Thronson, H.A., Lada, C.J., Hewagana, T., 1985, *ApJ* 297, 662
- Vacca, W.D., Garmany, C.D., Shull, J.M., 1996, *ApJ* 460, 914
- Verstraete, L., Pech, C., Moutou, C., Sellgren, K., Wright, C.M., Giard, M., Léger, A., Timmermann, R., Drapatz, S., 2001, *A&A* 372, 981
- Weingartner, J.C., Draine, B.T., 2001, *ApJ* 553, 581
- Whitworth, A.P., Bhattal, A.S., Chapman, S.J., Disney, M.J., Turner, J.A., 1994, *MNRAS* 268, 291
- Wood, D.O.S., Churchwell, E., 1989, *ApJ* 340, 265
- Wouterloot, J.G.A., Brand, J., 1989, *A&AS* 80, 149
- Wouterloot, J.G.A., Brand, J., Fiegle, K., 1993, *A&AS* 98, 589

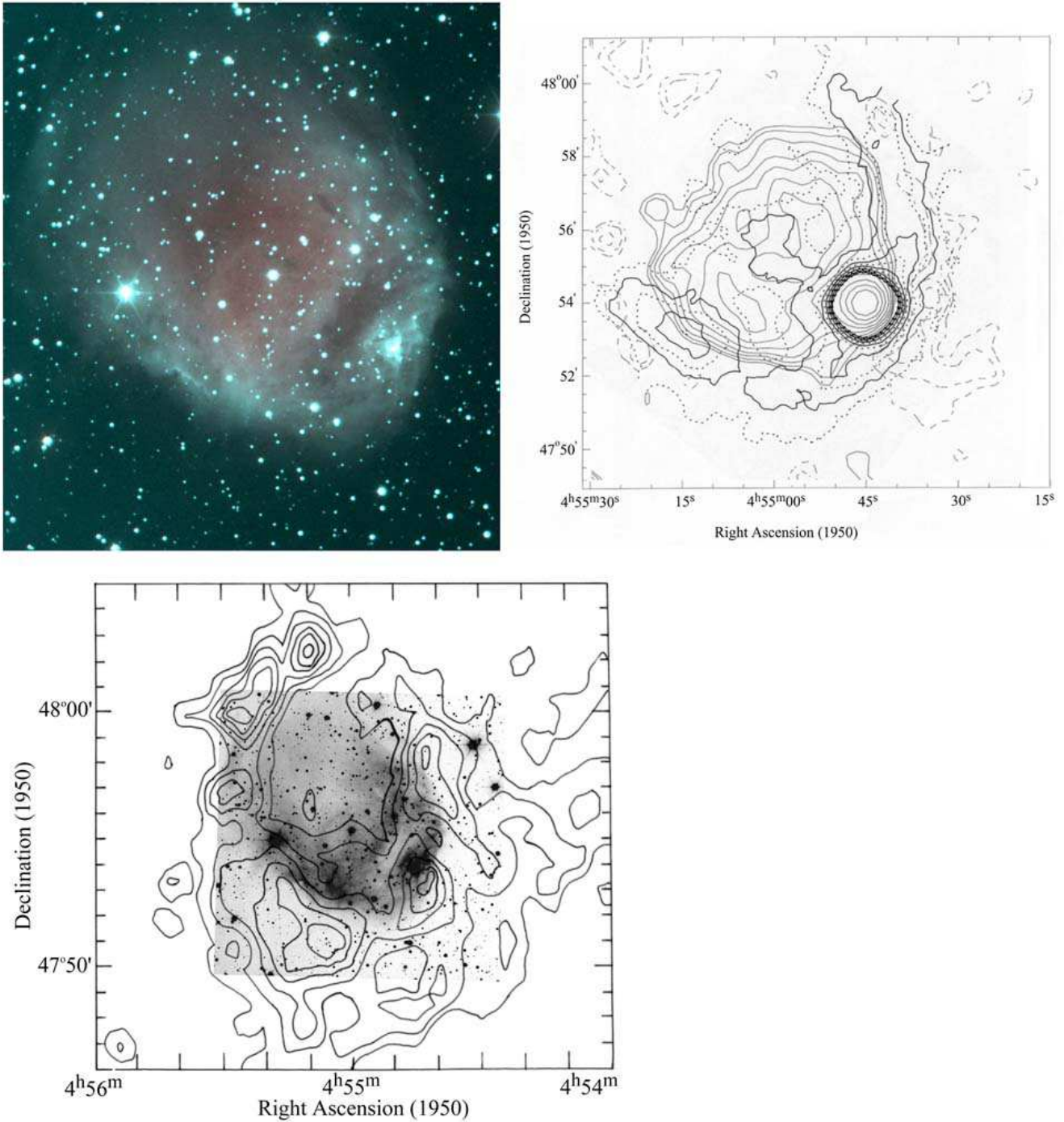


Fig. 2. **a)** Composite colour image of Sh 217 in the optical; same characteristics as Fig. 1a. The size of the field is $10'.25 \times 11'.25$. **b)** The black contours (solid and dotted), drawn from the MSX $8.3 \mu\text{m}$ image, are superimposed on the radio continuum map of Sh 217 (grey contours); the radio map is from the NVSS survey at 1.4 GHz (Condon et al. 1998). Only those MSX radiance contours in the range from 0.6 to $3.0 \times 10^{-6} \text{ W m}^{-2} \text{ sr}^{-1}$ are drawn; the radiance peaks at $30 \times 10^{-6} \text{ W m}^{-2} \text{ sr}^{-1}$ in the direction of the UC H II region. Note the half-ring of PAH emission surrounding the H II region and the good alignment, along the line of sight, of the radio and MSX ultracompact sources. **c)** Integrated H I emission associated with Sh 217 covering the LSR radial velocity range from -15.1 km s^{-1} to -20.1 km s^{-1} . The H I emission is from Roger & Leahy (1993). The H I contours are superimposed on the DSS2-red frame of Sh 217

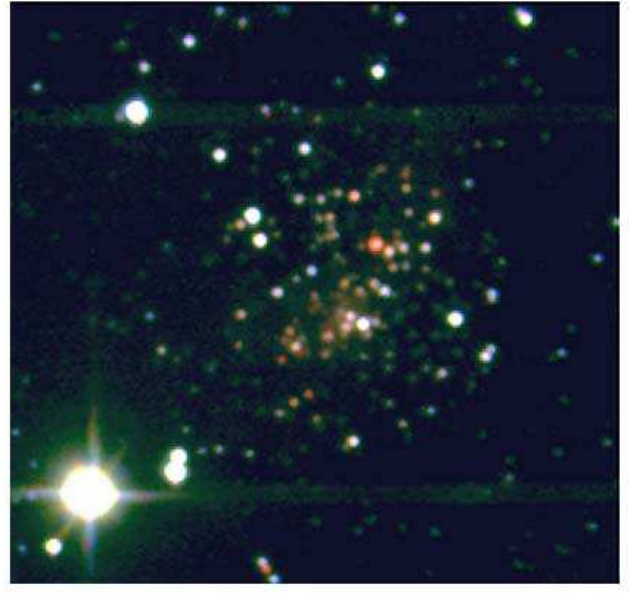
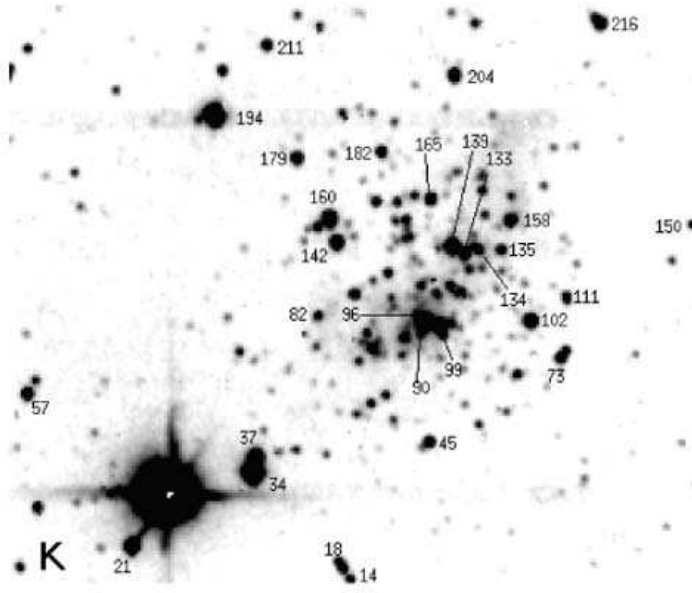


Fig. 3. **a)** K frame of the Sh 219 field. The frame size is $3'35 \times 2'8$. North is up, east is to the left. The stars discussed in the text are identified by their numbers in Table 3. **b)** JHK colour composite of the cluster associated with Sh 219 (blue for J , green for H and red for K)

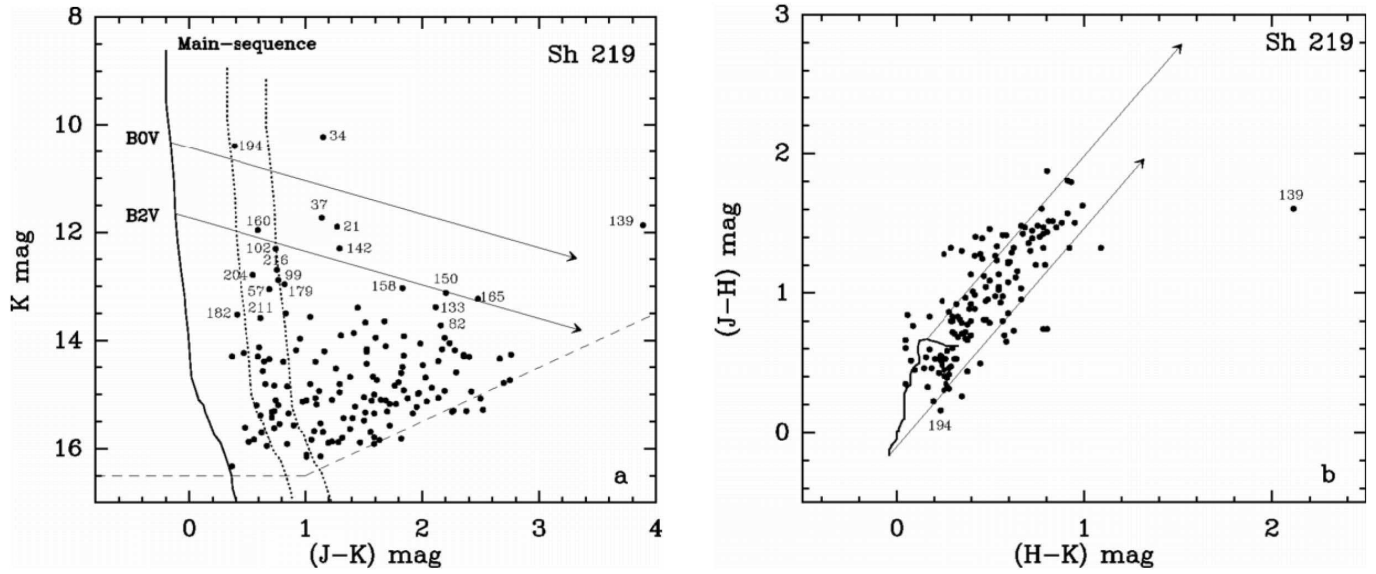


Fig. 4. **a)** The K versus $J-K$ magnitude-colour diagram of stars in the Sh 219 field. The main sequence is from Vacca et al. (1996) for O stars and from Schmidt-Kaler (1982) for later spectral types. The main sequence is drawn for a distance of 5 kpc, and for visual extinctions of zero (solid curve), 3 and 5 mag (dotted curves). The dashed lines show our detection limits. Reddening lines are drawn originating from B0V and B2V stars; they correspond to a visual extinction of 20 mag and the standard extinction law of Mathis (1990) with $R_V = 3.1$. **b)** The $(J-H)$ versus $(H-K)$ colour-colour diagram. The main sequence and the reddening lines corresponding to a visual extinction of 20 mag are shown as in Fig. 4a

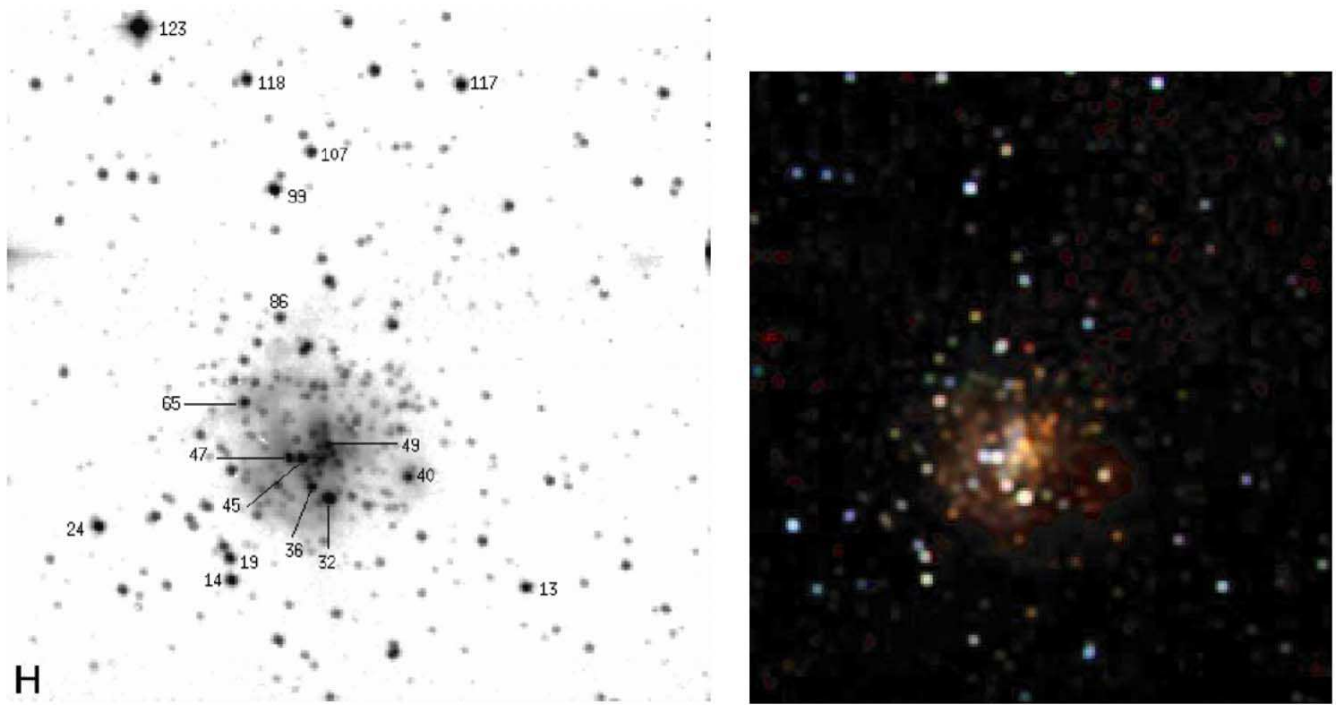


Fig. 5. **a)** *H* frame of the Sh 217 field. The field size is $3'.3 \times 3'.4$. North is up, east is to the left. The stars discussed in the text are identified by their numbers from Table 4. **b)** Composite colour image of the young stellar cluster observed at the periphery of Sh 217. *J* is blue, *H* is green and *K* is red